Applied Mathematics & Information Sciences
An International Journal

http://dx.doi.org/10.18576/amis/160507

Numerical Analysis of a Spatio-Temporal bi Modal Coronavirus Disease Pandemic

A. F. Koura[1], *K. R. Raslan*[2], *Khalid K. Ali*[2,*] *and M. A. Shaalan*[3]

[1]Basic Science Department, Al-Safwa High Institute of Engineering, Egypt
[2]Mathematics Department, Faculty of Science, Al-Azhar University, Nasr-City, Cairo, Egypt
[3]Basic Science Department, Higher Technological Institute, $10^{th}$of Ramadan City, Egypt

Received: 2 Mar. 2022, Revised: 2 Jun. 2022, Accepted: 23 Jul. 2022
Published online: 1 Sep. 2022

Abstract: In this article, we introduce a numerical study for a spatio temporal bi-modal of covid-19 mathematical model. The temporal only model consists of a system of five ordinary differential equations and spatio-temporal model consists of a system of five partial differential equations in time and space. We will discuss the stability region to get good selection of parameters. Also, we will apply the effective method of centeral finite difference (CFD) and study stability and consistency of this scheme then we will discuss the graphical numerical results of the presented models and the behavior of this model.

Keywords: Bi modal Covid-19 model, CFD method, Spatio-temporal, Stability

1 Introduction

In recent years, many researchers have studied the analytical and numerical solutions of some differential equations, ordinary and partial that describe some physical, engineering, and other phenomena. Coronavirus belongs to great number of viruses that has infected millions of people all over the world, the infectious pandemic have worth effects on the health and also on economy. Therefore, the study of the dynamics of transmission of the virus is great significant. Rafiq et al. [1] studied (SITR) dynamical model of Covid 19 with bimodal virus transmission in inhabitants of a state.This model merges the possible treatment measures of Covid-19 vaccines and suggested a new structure to keep numerical scheme for this model which generate an actual solutions of the SITR bi-modal nonlinear model. They found that human may face destructive effectiveness of pandemic if treatment measures are not carried out accurately. Kouidere et al. [2] introduced a mathematical model of Covid-19 provided three controls which represent sensitization and prevention, lock-down, diagnosis and observation in order to minimize the number of infected humans and suffered from serious complications. They applied the results of the control theory to obtain the characterizations of the optimal controls. The numerical simulation of the obtained results using Pontryagin's maximum principle showed the effect of the control strategies. In [3] Zakary et al. estimated the evolution of covid-19 viruse in countries that apply quarantine strategy as they presented a new mathematical model which described this situation.They used real data in Moroco to find the parameters in this model, also investigated an optimal control to reduce the numbers of people under risk who underestimate the quarantine. In [4] Kyrychko et al. modified age-structured mathematical model for covid-19 in Ukraine. This model assumed that people who have recovered from infection with covid-19 have immunity against this virus for the remaining time of the epidemic, also provided a forecast for the dynamics of covid-19 and explored the impact of lock down on the number of infections and deaths. Khoshnaw et al. in [5] suggested a new mathematical modeling for research of covid-19 and developments. They discussed The dynamics of model with some computational simulations. In [6] Roosa et al. used phenomenological models to generate forecasts of the cumulative number of confirmed cases that have been reported in Hubei province by collecting daily reports. Chayu Yang and Jin Wang in [7] proposed a mathematical model to describes ways of infection transmission. They analyzed this model and presented its application using

* Corresponding author e-mail: khalidkaram2012@yahoo.com

reported data. Their results deduced that corona infection would remain endemic, which presuppose long time of disease prevention and interference programs.Also in [8] D.Fanelli and F. Piazza analyzed the temporal dynamics of covid-19 virus in three different countries in time window and suggested that simple mean-eld models can be used to gather a preview of the spreading of this virus, and remarkably altitude and peak time of infected individuals. In [9] K. Liang Compared the new spread specifications of Covid-19 with those of SARS and Middle East Respiratory Syndrome and introduced a dynamic mathematical model of diseases to analyze the spread of covid-19, SARS and MERS by using nonlinear fitting. Sanchez et al. [10] presented simplified mathematical model of covid-19 that presents the dynamics of this virus in four different cases depending on the contact rate between individuals. Ahmed et al. in [11] presented a two dimensional space SIR reaction diffusion model and numerically solved it to study the behavior of this model using three different methods. Tang et al. devised a deterministic compartmental model based on the succession of the morbidness, estimated its reproduction number and studied sensitivity analysis on it [12]. Mammeri et al. [13] established model that describe the average daily movement of exhibitors and no visible symptoms for controlling the spread of the COVID-19 virus. They studied system of partial differential equations to determine the basic reproduction number. Then, they explained the spread of COVID-19 from March 16 to June 16 by making numerical simulations that concentrated on a combination of level-set and fnite difference. Finally, they compared unlocking scenarios according to a variation of distancing, or partially spatial lockdown. Nazarimehr et al. [14] investigated an epidemiology model for the development of Covid-19. They studied the spread of covid-19 through different sub-groups of society. They utilized early warning indicators to predict the bifurcation points in the system. They also investigated the different dynamics of the entire society by pairing these sub-groups. Nadim et al. [15] considered a mathematical model on the transmission of Covid-19 with the impact of the incomplete lockdown. They used the method of next generation matrix to calculate the basic reproduction number. They noticed that the model of Covid-19 transmission has backward bifurcation and showed that backward bifurcation did not occur under the perfect lockdown scenario. Nguiwa et al. [16] studied the effect of a fractional-order model of the cholera epidemic in Mayo-Tsanaga Department. They derived the basic reproduction number that describe the extinction and persistence of infection. They found that the parameter related to vaccination and therapeutic treatment is more effecting on the model. They supported the theoretical results by numerical simulations which also indicates the use of vaccination in the endemic area. [17] Xiao-Ping Li et al. used the fixed-point approach to study the existence of the covid-19 model and applied Newton polynomial and Adams Bashforth approaches to calculate the parameters that explain system behavior. Ahmed et al. [18] investigated the spread of new Covid-19 which is an extension of the Covid-19 SEIR model. They performed the stability analysis to attain the equilibrium points of the model. They studied the effect of parameters numerically and observed that the results of random motion of individuals have a considerable impact on the observed dynamics and provided some strategies to control virus spread.

This article is arranged as follows: In section 2, we present a mathematical formulation for the Covid-19 temporal and spatio-temporal models. We investigate equilibrium points and stability region as shown in sections 3. In section 4, we introduce numerical solutions for the spatio-temporal model of COVID-19 via finite difference. In section 5, we discuss the stability and consistency of the numerical scheme.

2 Mathematical Formulation

For spacious interest of mathematical modeling for epidemiological system like Cov-19, the effectiveness of movement of people from one place to another is not taken into account. This motivates researchers to present a more factual model of Cov-19 having a nonlinear occurrence rate in the spatiotemporal case.

Temporal model:

$$\begin{aligned}
\frac{dS_a}{dt} &= \Lambda_a - \alpha_a I S_a - \delta S_a,\\
\frac{dS_b}{dt} &= \Lambda_b - \alpha_b I S_b - \delta S_b,\\
\frac{dI}{dt} &= I(\alpha_a S_a + \alpha_b S_b) - I(\gamma - \delta),\\
\frac{dT}{dt} &= \gamma I - T(\beta + \delta),\\
\frac{dR}{dt} &= \beta T - \delta R.
\end{aligned} \tag{1}$$

Spatiotemporal model:

$$\begin{aligned}
\frac{\partial S_a}{\partial t} &= C_1 \frac{\partial^2 S_a}{\partial x^2} + \Lambda_a - \alpha_a I S_a - \delta S_a,\\
\frac{\partial S_b}{\partial t} &= C_2 \frac{\partial^2 S_b}{\partial x^2} + \Lambda_b - \alpha_b I S_b - \delta S_b,\\
\frac{\partial I}{\partial t} &= C_3 \frac{\partial^2 I}{\partial x^2} + I(\alpha_a S_a + \alpha_b S_b) - I(\gamma - \delta),\\
\frac{\partial T}{\partial t} &= C_4 \frac{\partial^2 T}{\partial x^2} + \gamma I - T(\beta + \delta),\\
\frac{\partial R}{\partial t} &= C_5 \frac{\partial^2 R}{\partial x^2} + \beta T - \delta R.
\end{aligned} \tag{2}$$

At any time $t \in [0,\infty)$, $S_a(t)$ represents the number of susceptible people that are not infected , $S_b(t)$ represents

the number susceptible people from the elderly and those with chronic diseases, $I(t)$ represents the number of actually infected people with Cov-19, $T(t)$ represents the number of people undergoing treatment and $R(t)$ represents the number of recovered people after treatment.
In this work, the parameters are described as follows: Λ_a, Λ_b indicates the influx rate of susceptible class S_a and susceptible class S_b respectively,α_a, α_b represents the infection rate of susceptible class S_a and susceptible class S_b respectively ,δ natural death rate, γ treatment rate and β refers to recovery rate.
Consider the Spatiotemporal model (2) with initial conditions,

$$\begin{aligned}
S_a(0,x) &= \begin{cases} 0.5x & 0 \le x \le 0.5 \\ 0.5(1-x) & 0.5 \le x \le 1, \end{cases} \\
S_b(0,x) &= \begin{cases} 0.2x & 0 \le x \le 0.5 \\ 0.2(1-x) & 0.5 \le x \le 1, \end{cases} \\
I(0,x) &= \begin{cases} 0.1x & 0 \le x \le 0.5 \\ 0.1(1-x) & 0.5 \le x \le 1, \end{cases} \\
T(0,x) &= \begin{cases} 0.1x & 0 \le x \le 0.5 \\ 0.1(1-x) & 0.5 \le x \le 1, \end{cases} \\
R(0,x) &= \begin{cases} 0.1x & 0 \le x \le 0.5 \\ 0.1(1-x) & 0.5 \le x \le 1. \end{cases}
\end{aligned} \tag{3}$$

and homogeneous Neumann boundary conditions,

$$\begin{aligned}
\frac{\partial S_a(t,0)}{\partial x} &= \frac{\partial S_a(t,1)}{\partial x} = 0, \\
\frac{\partial S_b(t,0)}{\partial x} &= \frac{\partial S_b(t,1)}{\partial x} = 0, \\
\frac{\partial I(t,0)}{\partial x} &= \frac{\partial I(t,1)}{\partial x} = 0, \\
\frac{\partial T(t,0)}{\partial x} &= \frac{\partial T(t,1)}{\partial x} = 0, \\
\frac{\partial R(t,0)}{\partial x} &= \frac{\partial R(t,1)}{\partial x} = 0.
\end{aligned} \tag{4}$$

The spatiotemporal system (2) with initial conditions (3) and boundary conditions (4)is the one we will apply the numerical method to get numerical solution.

3 Equilibrium points and stability

In this section, we study equilibrium points stability for both temporal model (1) and spatiotemporal model (2).

3.1 Temporal only model

Suppose that disease-free equilibrium point is E^0 and the endemic equilibrium point is E^* for temporal model (1) deduced in [1]

$$E^0 = (\frac{\Lambda_a}{\delta}, \frac{\Lambda_b}{\delta}, 0, 0, 0), \tag{5}$$

$$E^* = (S_a^*, S_b^*, I^*, T^*, R^*), \tag{6}$$

also in [1] the Jacobian of the system (1) at E^0 given by:

$$J_0 = \begin{bmatrix} -\delta & 0 & -\alpha_a\Lambda_a/\delta & 0 & 0 \\ 0 & -\delta & -\alpha_b\Lambda_b/\delta & 0 & 0 \\ 0 & 0 & (\alpha_a\Lambda_a + \alpha_b\Lambda_b)/\delta - (\delta+\gamma) & 0 & 0 \\ 0 & 0 & \gamma & -(\delta+\beta) & 0 \\ 0 & 0 & 0 & \beta & -\delta \end{bmatrix}, \tag{7}$$

and the Jacobian of the system (1) at E^* given by:

$$J_* = \begin{bmatrix} -\frac{\Lambda_a}{S_a^*} & 0 & -\alpha_a S_a^* & 0 & 0 \\ 0 & -\frac{\Lambda_b}{S_b^*} & -\alpha_b S_b^* & 0 & 0 \\ \alpha_a I^* & \alpha_b I^* & 0 & 0 & 0 \\ 0 & 0 & \gamma & -(\delta+\beta) & 0 \\ 0 & 0 & 0 & \beta & -\delta \end{bmatrix}. \tag{8}$$

Solving the characteristic equation for (7) to get its eigenvalues we get that the temporal only system 1 is locally asymptotically stable if and only if

$$\frac{1}{\delta}(\alpha_a\Lambda_a + \alpha_b\Lambda_b) - \delta - \gamma < 0,$$

to get stability conditions for endemic equilibrium point E^* it is difficult to solve the characteristic equation for J_* and get condition from its eigenvalues, so we numerically solve it and using the parameters $\Lambda_a = 0.2; \Lambda_a = 0.05; \delta = 0.25; \beta = 0.3; \alpha_a = 0.3; \alpha_b = 0.6; \gamma = 0.1$, we found that all eigenvalues are negative which leads to the achievement Roth-Hertz stability condition.

3.2 spatiotemporal model

Assume that the spatiotemporal model (2) has coefficients not equal zero $C_1, C_2,$
C_3, C_4, C_5, and has an equilibrium point that takes the form $(\bar{S}_a, \bar{S}_b, \bar{I}, \bar{T}, \bar{R})$.
To linearize the system we will apply small perturbations $\hat{S}_a = S_a - \bar{S}_a, \hat{S}_b = S_b - \bar{S}_b, \hat{I} = I - \bar{I}, \hat{T} = T - \bar{T}, \hat{R} = R - \bar{R}$, we get

$$\begin{aligned}
\frac{\partial \hat{S}_a}{\partial t} &= C_1\frac{\partial^2 \hat{S}_a}{\partial x^2} + d_{11}\hat{S}_a + d_{12}\hat{S}_b + d_{13}\hat{I} + d_{14}\hat{T} + d_{15}\hat{R} \\
\frac{\partial \hat{S}_b}{\partial t} &= C_2\frac{\partial^2 \hat{S}_b}{\partial x^2} + d_{21}\hat{S}_a + d_{22}\hat{S}_b + d_{23}\hat{I} + d_{24}\hat{T} + d_{25}\hat{R}, \\
\frac{\partial \hat{I}}{\partial t} &= C_3\frac{\partial^2 \hat{I}}{\partial x^2} + d_{31}\hat{S}_a + d_{32}\hat{S}_b + d_{33}\hat{I} + d_{34}\hat{T} + d_{35}\hat{R}, \\
\frac{\partial \hat{T}}{\partial t} &= C_4\frac{\partial^2 \hat{T}}{\partial x^2} + d_{41}\hat{S}_a + d_{42}\hat{S}_b + d_{43}\hat{I} + d_{44}\hat{T} + d_{45}\hat{R}, \\
\frac{\partial \hat{R}}{\partial t} &= C_5\frac{\partial^2 \hat{R}}{\partial x^2} + d_{51}\hat{S}_a + d_{52}\hat{S}_b + d_{53}\hat{I} + d_{54}\hat{T} + d_{55}\hat{R},
\end{aligned} \tag{9}$$

assume that the solution of system (9) given by

$$\begin{pmatrix} \hat{S}_a \\ \hat{S}_b \\ \hat{I} \\ \hat{T} \\ \hat{R} \end{pmatrix} = \begin{pmatrix} S_{a_0} \\ S_{b_0} \\ I_0 \\ T_0 \\ R_0 \end{pmatrix} * e^{wt - i\theta x}, \tag{10}$$

where $S_{a_0}, S_{b_0}, I_0, T_0, R_0$ have small values. Substituting with (10) into system (9), we get

$$\varpi \begin{pmatrix} \hat{S}_a \\ \hat{S}_b \\ \hat{I} \\ \hat{T} \\ \hat{R} \end{pmatrix} = \begin{pmatrix} d_{11} - \theta^2 C_1 & d_{12} & d_{13} & d_{14} & d_{15} \\ d_{21} & d_{22} - \theta^2 C_2 & d_{23} & d_{24} & d_{25} \\ d_{31} & d_{32} & d_{33} - \theta^2 C_3 & d_{34} & d_{35} \\ d_{41} & d_{42} & d_{43} & d_{44} - \theta^2 C_4 & d_{45} \\ d_{51} & d_{52} & d_{53} & d_{54} & d_{55} - \theta^2 C_5 \end{pmatrix} * \begin{pmatrix} \hat{S}_a \\ \hat{S}_b \\ \hat{I} \\ \hat{T} \\ \hat{R} \end{pmatrix} \tag{11}$$

where, the values of d_{ij} in (11) are determined from Jacobian J_0 at disease-free equilibrium point, Jacobian J_* at endemic equilibrium point, θ is the wave number and ϖ is growth rate of the disturbances around the chosen equilibrium point. According to the sign of the real parts of ϖ the stability of the equilibrium point of the spatiotemporal model (2) is determined in three cases: first case real parts of ϖ less than zero the equilibrium point of the model (2) is locally asymptotic stable, while second and third cases the model (2) is unstable if ϖ equal to zero and ϖ is imaginary, respectively.

3.3 Region of stability

The region of stability of the disease-free equilibrium and endemic points shown for (α_a, α_b, γ) in figure 1 and figure 2, we fix the values of other parameters as follows $\Lambda_a = 0.2; \Lambda_a = 0.05; \delta = 0.25; \beta = 0.3$.

Figure 1a examines the effects of (α_a, α_b, γ) at disease-free equilibrium point, while Figure 1b, c, d illustrates the projection of stability region (α_a,α_b) with fixed γ at $0.1, 0.5$ and 0.7 respectively. We observe that α_a and α_b maintain their stability at large value if γ.

Figure 2a examines the effects of (α_a,α_b, γ) at disease free equilibrium point, while Figure 2b, c, d illustrates the projection of stability region (α_a, α_b) with fixed γ at $0.1, 0.5$ and 0.7 respectively. We observe that α_a and α_b maintain their stability at small value of γ.

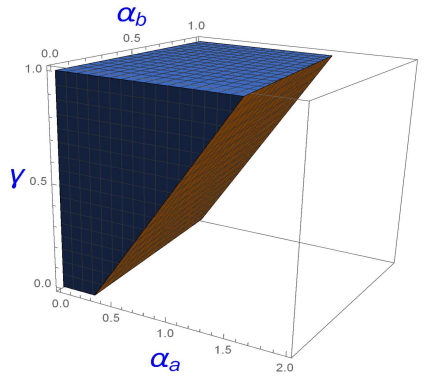

(a) (α_a,α_b,γ) space

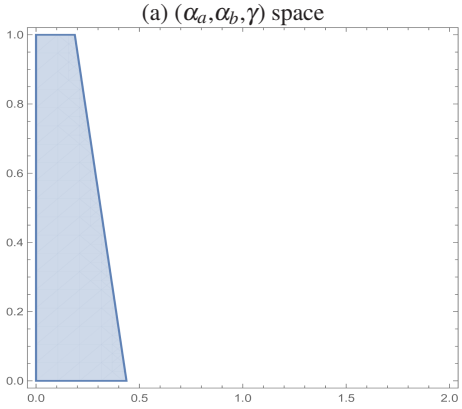

(b) (α_a,α_b,$\gamma = 0.1$)

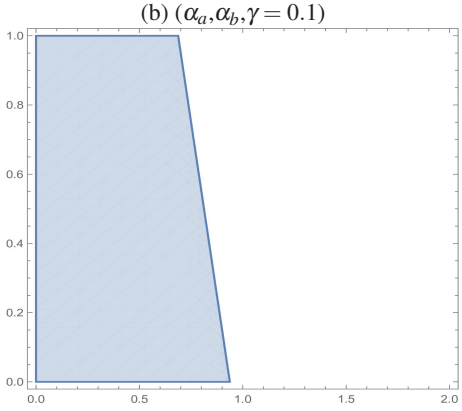

(c) (α_a,α_b,$\gamma = 0.5$)

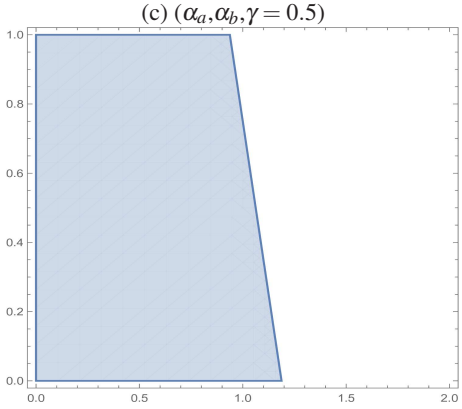

(d) (α_a,α_b,$\gamma = 0.7$)

Fig. 1: stability region for disease free equilibrium point

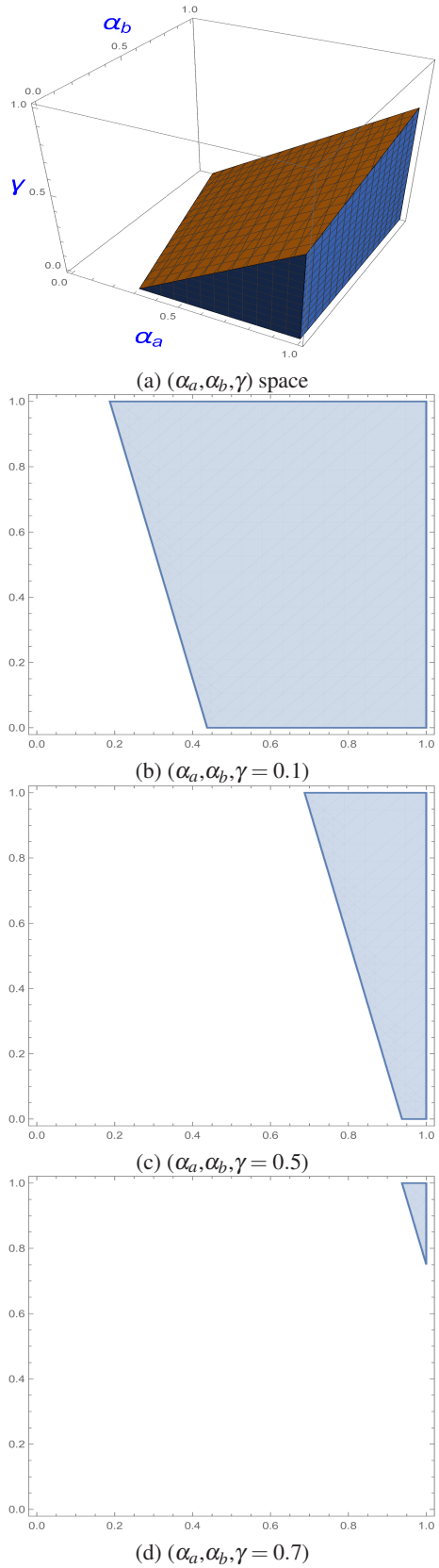

(a) $(\alpha_a, \alpha_b, \gamma)$ space

(b) $(\alpha_a, \alpha_b, \gamma = 0.1)$

(c) $(\alpha_a, \alpha_b, \gamma = 0.5)$

(d) $(\alpha_a, \alpha_b, \gamma = 0.7)$

Fig. 2: stability region for endemic equilibrium point

4 Numerical solution and results

In this section, we present a numerical method of spatiotemporal model (2) and divide the domain of $x \in [0,1]$ and $t \in [0,300]$ into 100×300 cubes with step size $h = 0.1$ and $\tau = 1$.
We apply finite difference using

$$\begin{aligned} \frac{\partial f(t,x)}{\partial t} &= \frac{f_i^{n+1} - f_i^n}{\tau}, \\ \frac{\partial^2 f(t,x)}{\partial x^2} &= \frac{f_{i-1}^{n+1} - 2f_i^{n+1} + f_{i+1}^{n+1}}{h^2}, \\ \frac{\partial f(t,x)}{\partial x} &= \frac{f_{i+1}^n - f_{i-1}^n}{2h}, \end{aligned} \tag{12}$$

and then discretization the system (2) and its boundary conditions(4) we get the following results,

$$\begin{aligned} (S_a)_i^{n+1} =& (S_a)_i^n + \frac{\tau C_1}{h^2}((S_a)_{i+1}^{n+1} - 2(S_a)_i^{n+1} + (S_a)_{j-1}^{n+1}) \\ &+ \tau\lambda_a - \tau\alpha_a I_i^n (S_a)_i^{n+1} - \tau\delta(S_a)_i^{n+1}, \end{aligned} \tag{13}$$

$$\begin{aligned} (S_b)_i^{n+1} =& (S_b)_i^n + \frac{\tau C_2}{h^2}((S_b)_{i+1}^{n+1} - 2(S_b)_i^{n+1} + (S_b)_{j-1}^{n+1}) \\ &+ \tau\Lambda_b - \tau\alpha_b I_i^n (S_b)_i^{n+1} - \tau\delta(S_b)_i^{n+1}, \end{aligned} \tag{14}$$

$$\begin{aligned} I_i^{n+1} =& I_i^n + \frac{\tau C_3}{h^2}(I_{i+1}^{n+1} - 2I_i^{n+1} + I_{j-1}^{n+1}) + \tau I_i^{n+1}(\alpha_a (S_a)_i^n \\ &+ \alpha_b (S_b)_i^n) - \tau I_i^{n+1}(\gamma - \delta), \end{aligned} \tag{15}$$

$$\begin{aligned} T_i^{n+1} =& T_i^n + \frac{\tau C_4}{h^2}(T_{i+1}^{n+1} - 2T_i^{n+1} + T_{j-1}^{n+1}) + \tau\gamma I_i^n \\ &- \tau(\beta + \delta)T_i^{n+1}, \end{aligned} \tag{16}$$

$$\begin{aligned} R_i^{n+1} =& R_i^n + \frac{\tau C_5}{h^2}(R_{i+1}^{n+1} - 2R_i^{n+1} + R_{j-1}^{n+1}) + \tau\beta T_i^n \\ &- \tau\delta R_i^{n+1}. \end{aligned} \tag{17}$$

By solving the above equations $(13-17)$ with the values of parameters which were extracted and discussed in section 3.
Figure 3 shows the numerical solution at a disease-free equilibrium state which converges to the uniform steady state at the selected parameters, the numerical results have good agreement with the stability region analysis as shown in section 3. In Figure 3a, b $S_a(x,t)$ and $S_a(x,t)$ approach from 0.8 and 0.2, respectively and represent the whole number of population which is equal 1. Also we see at this equilibrium point the values of I, T and R become zero in figure 3c, d, e, respectively.
Figure 4 shows the numerical solution at endemic equilibrium state which converges to the uniform steady state at the selected parameters, the numerical results in Figure 4a, b, c, d, e for $S_a(x,t)$, $S_a(x,t)$, I, T and R comes to its endemic equilibrium point which is good agreement with the stability region analysis as shown in section 3.

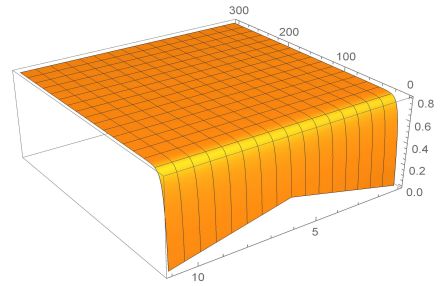

(a) $S_a(t,x)$

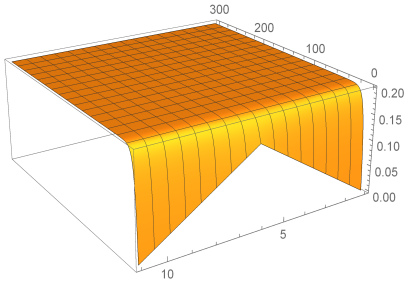

(b) $S_b(t,x)$

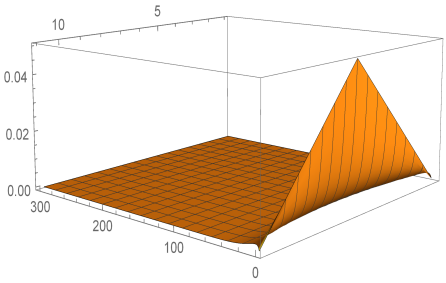

(c) $I(t,x)$

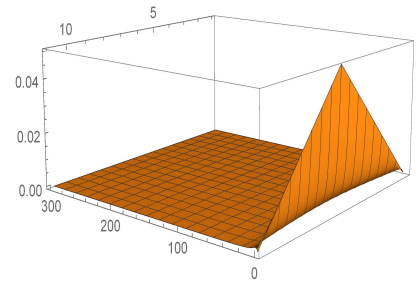

(d) $T(t,x)$

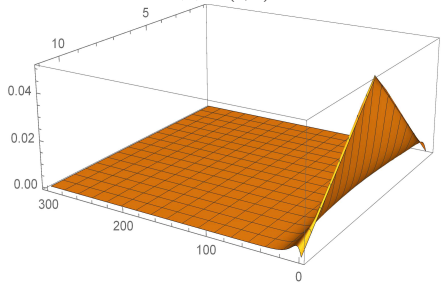

(e) $R(t,x)$

Fig. 3: Numerical simulation results for disease free equilibrium point

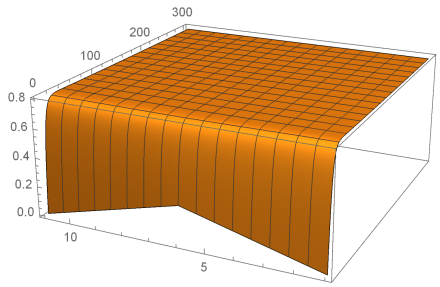

(a) $S_a(t,x)$

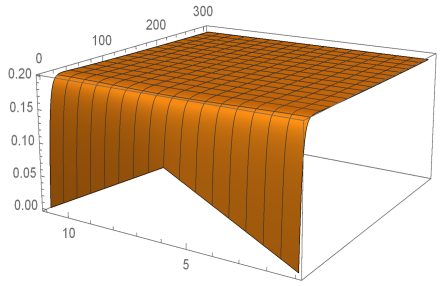

(b) $S_b(t,x)$

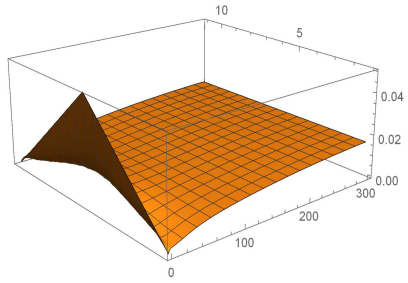

(c) $I(t,x)$

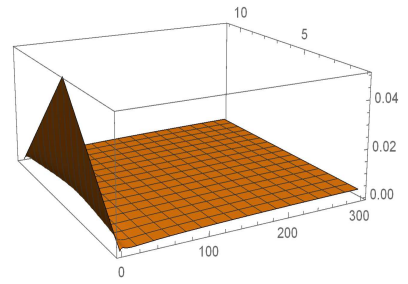

(d) $T(t,x)$

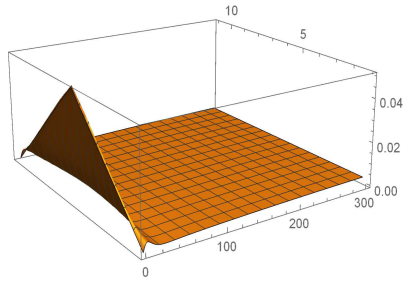

(e) $R(t,x)$

Fig. 4: Numerical simulation results for endemic equilibrium point

5 Stability of the numerical method

Theorem 1.*The presented numerical method has difference schemes* (13)-(17) *is conditionally stable.*

*Proof.*Using Von Neumann stability for the numerical method, we assume:

$$\begin{aligned}(S_a)_i^n &= \xi_1^n e^{Jk_{s_a}ih},\\ (S_a)_i^{n+1} &= \xi_1^{n+1} e^{Jk_{s_a}ih},\\ (S_a)_{i+1}^n &= \xi_1^n e^{Jk_{s_a}(i+1)h},\\ (S_a)_{i-1}^n &= \xi_1^n e^{Jk_{s_a}(i-1)h}.\end{aligned} \tag{18}$$

substitute from(18) in equation (13) we get the following relation,

$$\begin{aligned}\xi_1^{n+1}e^{Jk_{s_a}ih} = \xi_1^n e^{Jk_{s_a}ih} + \frac{\tau C_1}{h^2}(\xi_1^{n+1}e^{Jk_{s_a}(i+1)h}\\ -2\xi_1^{n+1}e^{Jk_{s_a}ih} + \xi_1^{n+1}e^{Jk_{s_a}(i-1)h}) + \tau\Lambda_a\\ -\tau\alpha_a I_i^n \xi_1^{n+1}e^{Jk_{s_a}ih}\tau\delta\xi_1^{n+1}e^{Jk_{s_a}ih},\end{aligned} \tag{19}$$

define amplification factor $G_1 = \frac{(S_a)_i^{n+1}}{(S_a)_i^n}$, we can compute G_1 by dividing equation (19) by $(S_a)_i^n$ we can obtain:

$$\begin{aligned}G_1 =& 1 + \frac{\tau C_1}{h^2}(Ge^{Jk_{s_a}h} - 2G + Ge^{-Jk_{s_a}h}) + \tau\Lambda_a - \tau\alpha_a I_i^n G\\ &-\tau\delta G,\end{aligned}$$

$$G = \frac{1}{1 + 4\frac{\tau C_1}{h^2}sin^2(\frac{k_{s_a}h}{2}) + \upsilon_a^{\cdot} + \tau\delta},$$

$$G_1 = \left|\frac{1}{1 + 4\frac{\tau C_1}{h^2}sin^2(\frac{k_{s_a}h}{2}) + \upsilon_a^{\cdot} + \tau\delta}\right| \leq 1, \tag{20}$$

similarly, repeating the previous steps to equations (14, 15, 16, 17) for $(S_b)_i^n, I_i^n, R_i^n$ and T_i^n with $(S_b)_i^n = \xi_2^n e^{Jk_{s_b}ih}$, $I_i^n = \xi_3^n e^{Jk_I ih}$, $R_i^n = \xi_4^n e^{Jk_R ih}$ and $T_i^n = \xi_5^n e^{Jk_T ih}$ respectively, we also obtain:

$$G_2 = \left|\frac{1}{1 + 4\frac{\tau C_2}{h^2}sin^2(\frac{k_{s_b}h}{2}) + \upsilon_b^{\cdot} + \tau\delta}\right| \leq 1, \tag{21}$$

$$G_3 = \left|\frac{1}{1 + 4\frac{\tau C_3}{h^2}sin^2(\frac{k_I h}{2}) + \tau(\delta + \gamma - \upsilon_I^{\cdot})}\right| \leq 1, \tag{22}$$

$$G_4 = \left|\frac{1}{1 + 4\frac{\tau C_4}{h^2}sin^2(\frac{k_T h}{2}) + \tau(\delta + \beta)}\right| \leq 1, \tag{23}$$

$$G_5 = \left|\frac{1}{1 + 4\frac{\tau C_5}{h^2}sin^2(\frac{k_R h}{2}) + \tau\delta}\right| \leq 1, \tag{24}$$

where $\upsilon_a^{\cdot} = \tau\alpha_a I_i^n$, $\upsilon_b^{\cdot} = \tau\alpha_b I_i^n$, where $\upsilon_I^{\cdot} = \alpha_a S_a + \alpha_b S_b$ and $J = \sqrt{-1}$.
So $G_i \leq 1$, $i = 1,2,3,4,5$ which is the necessary and sufficient condition for the error to remain bounded and maintain von Neumann stability for the numerical method.

6 Consistency of the numerical method

Theorem 2.*The difference schemes* (13)-(17) *of the proposed method have local truncation error* $O(h^2 + \tau)$.

*Proof.*Use Taylor expansion to prove that this numerical scheme second-order in x and first-order in t, for this we use:

$$\begin{aligned}\Phi_{S_a} =& \frac{(S_a)_i^{n+1} - (S_a)_i^n}{\tau} - \frac{C_1}{h^2}((S_a)_{i+1}^{n+1} - 2(S_a)_i^{n+1}\\ &+ (S_a)_{j-1}^{n+1}) - \Lambda_a + \alpha_a I_i^n (S_a)_i^{n+1} + \delta(S_a)_i^{n+1},\end{aligned}$$

$$\begin{aligned}\Phi_{S_a} =& (\frac{\partial S_a}{\partial t} + \frac{\tau}{2!}\frac{\partial^2 S_a}{\partial t^2} + \frac{\tau^2}{3!}\frac{\partial^2 S_a}{\partial t^2} + ...)\\ &- \frac{C_1}{h^2}(h^2(\frac{\partial^2 S_a}{\partial x^2} + 2\frac{h^2}{4!}\frac{\partial^4 S_a}{\partial x^2} + ...)) - \Lambda_a\\ &+ (\alpha_a I_i^n + \delta) * (S_{ai}{}^n + \tau\frac{\partial S_a}{\partial t} + \frac{\tau^2}{2!}\frac{\partial^2 S_a}{\partial t^2}\\ &+ \frac{\tau^3}{3!}\frac{\partial^2 S_a}{\partial t^2} + ...),\end{aligned}$$

$$\begin{aligned}\Phi_{S_a} =& \frac{\partial S_a}{\partial t} - \frac{C_1}{h^2}(h^2\frac{\partial^2 S_a}{\partial x^2}) - \Lambda_a + (\alpha_a I_i^n + \delta) * (S_{ai}{}^n)\\ &- \frac{C_1 h^2}{12}(\frac{\partial^4 S_a}{\partial x^4}) + \tau((\alpha_a I_i^n + \delta)\frac{\partial S_a}{\partial t} + ...),\end{aligned}$$

$$\Phi_{S_a} = -\frac{C_1 h^2}{12}(\frac{\partial^4 S_a}{\partial x^4}) + \tau((\alpha_a I_i^n + \delta)\frac{\partial S_a}{\partial t} + ...),$$

which devolve to zero as τ,h become zero.
Also we can obtain the relations of S_b , I, R and T using the previous steps as the following

$$\begin{aligned}\Phi_{S_b} &= -\frac{C_2 h^2}{12}(\frac{\partial^4 S_b}{\partial x^4}) + \tau((\alpha_b I_i^n + \delta)\frac{\partial S_b}{\partial t} + ...),\\ \Phi_I &= -\frac{C_3 h^2}{12}(\frac{\partial^4 I}{\partial x^4}) + \tau((\gamma - \delta)\frac{\partial I}{\partial t} + ...),\\ \Phi_T &= -\frac{C_4 h^2}{12}(\frac{\partial^4 T}{\partial x^4}) + \tau((\beta + \delta)\frac{\partial T}{\partial t} + ...),\\ \Phi_R &= -\frac{C_5 h^2}{12}(\frac{\partial^4 R}{\partial x^4}) + \tau(\delta\frac{\partial R}{\partial t} + ...),\end{aligned}$$

which also go to zero as as τ, h become zero. For this the order of accuracy of this numerical method is $O(h^2 + \tau)$.

7 Conclusion

A numerical study for a spatio temporal bi-modal of covid-19 mathematical model in time and space have been introduced. We discussed the stability region and get good selection of parameters, then we apply the effective centeral finite difference method (CFD). Stability and consistency of this scheme was studied then we discussed the graphical numerical results of the presented models that show the behavior of the spread of the epidemic and support the validity of numerical scheme.

Acknowledgement

We would like to thank the reviewers for helpful and constructive comments, which have made great contributions to the improvement of the paper.

Conflict of Interest The authors declare that they have no conflict of interest.

References

[1] M. Rafik , J. Ali , M. B. Riaz and J. Awrejcewicz, Numerical analysis of a bi-modal COVID-19 sitr model, Alexandria Engineering Journal, **61**(1), 227-235 (2022).
[2] A.Kouidere, B. Khajji, A. El Bhih and O. Balatif, A mathematical modeling with optimal control strategy of transmission of COVID-19 pandemic virus, Commun. Math. Biol. Neurosci, 2020 (2020).
[3] O. Zakary, S. Bidah, M. Rachik and H. Ferjouchia, Mathematical Model to Estimate and Predict the COVID-19 Infections in Morocco: Optimal Control Strategy, Journal of Applied mathematics, 2020 (2020).
[4] Y. N. Kyrychko, K. B. Blyuss and I. Brovchenko, Mathematical modelling of dynamics and containment of COVID-19 in Ukraine, Scientific reports, **10**(1), 1-11 (2020).
[5] S. H. A. Khoshnaw, R. Salih and S. Sulaimany, Mathematical Modelling for Coronavirus Disease (COVID-19) in Predicting Future Behaviours and Sensitivity Analysis, Mathematical Modelling of Natural Phenomena, **15**, 33 (2020).
[6] K. Roosa, Y. Lee, R. Luo, A. Kirpich, R. Rothenberg,J.M. Hyman, G. Chowell and P.Yan, Real-time forecasts of the COVID-19 epidemic in China from February 5th to February 24th, 2020, Infectious Disease Modelling, **5**, 256-263 (2020).
[7] C.Yang, J. Wang, A mathematical model for the novel coronavirus epidemic in Wuhan, China, Mathematical biosciences and engineering: MBE, **17**(3), 2708 (2020).
[8] D.Fanelli and F. Piazza, Analysis and forecast of COVID-19 spreading in China, Italy and France, Chaos, Solitons & Fractals, **134**, 109761 (2020).
[9] K. Liang, Mathematical model of infection kinetics and its analysis for COVID-19, SARS and MERS , Infection, Genetics and Evolution, **82**, 104306 (2020).
[10] Y. G. Sanchez, Z. Sabir and J. N L. G. Guirao, Design of a nonlinear SITR fractal model based on the dynamics of a novel coronavirus (COVID-19), Fractals, **28**(8), 2040026 (2020).
[11] N. Ahmed, M. Ali, M. Rafiq, I. Khan, K. S. Nisar, M.A.Rehman and M.O. Ahmad, A numerical efficient splitting method for the solution of two dimensional susceptible infected recovered epidemic model of whooping cough dynamics: Applications in bio-medical engineering, Computer Methods and Programs in Biomedicine, **190**, 105350 (2020).
[12] B. Tang, X. Wang, Q. Li, N. L. i. Bragazzi, S. Tang, J. Wu and Y. Xiao, Estimation of the Transmission Risk of the 2019-nCoV and Its Implication for Public Health Interventions ,Journal of clinical medicine, **9**(2), 462 (2020).
[13] Y. Mammeri, A reaction-diffusion system to better comprehend the unlockdown: Application SEIR-type model with diffusion to the spatispread of COVID-19 in France, Computational and Mathematical Biophysics, **8**(1), 102-113 (2020).
[14] F. Nazarimehr, V.T. Pham and T. Kapitaniak, Prediction of bifurcations by varying critical parameters of COVID-19, Nonlinear Dynamics, **101**(3), 1681-1692 (2020).
[15] S. S. Nadim and J.Chattopadhyay, Occurrence of backward bifurcation and prediction of disease transmission with imperfect lockdown: A case study on COVID-19, Chaos, Solitons & Fractals, **140**, 110163 (2020).
[16] T. Nguiwa, M. Justin, D. Moussa, G. Betchewe and A. Mohamadou, Dynamic Study of SIQR-B Fractional-Order Epidemic Model of Cholera with Optimal Control Strategies in Mayo-Tsanaga Department of Cameroon Far North Region, Biophysical Reviews and Letters, **15**(04), 237-273 (2020).
[17] Xiao-Ping Li, H. Al Bayatti, A. Din and A. Zeb, A vigorous study of fractional order COVID-19 model via ABC derivatives, Results in Physics, **29**, 104737, (2021).
[18] N. Ahmed, A. Elsonbaty, A. Raza, M. Rafiq and W. Adel, Numerical simulation and stability analysis of a novel reaction-diffusion COVID-19 model, Nonlinear Dynamics, **106**(2), 1293-1310 (2021).

A. F. Koura Received the M.Sc. degree in pure mathematics 2019, from mathematics department, faculty of science – Suez University – Suez –Egypt. Registered Ph.D. in Al-Azhar University - Cairo – Egypt in 2021 and still up to now.

Kamal R. Raslan received the M.Sc. and Ph.D. degrees from the Faculty of Science, Menoufia University and Al-Azhar University, Egypt, in 1996 and 1999, respectively. He is currently a full Professor of Mathematics with the Faculty of Science, Al-Azhar University, Egypt. He has authored/coauthored over 114 scientific papers in top-ranked International Journals and Conference Proceedings. His research interests include Numerical Analysis, Finite Difference Methods, Finite Element Methods, Approximation Theory, and Computational Mathematics.

Khalid K. Ali MSc in pure Mathematics, Mathematics Department 2015 from Faculty of Science, Al-Azhar University, Cairo, Egypt. Ph.D. in pure Mathematics 2018 from Faculty of Science, Al-Azhar University, Cairo, Egypt. He has authored/co-authored over 50 scientific papers in top-ranked International Journals and Conference Proceedings. His research interests include Numerical Analysis, Finite Difference Methods, Finite Element Methods, and Computational Mathematics.

M. A. Shaalan is working as a lecturer in the Department of Basic Science at Higher Technological Institute, Tenth of Ramadan City, Egypt. Earned his BSc and MSc degrees in Mathematics from Zagazig University, Egypt, in 2007 and 2014, respectively. Ph.D. in pure Mathematics 2019 from Faculty of Science, Al-Azhar University, Cairo, Egypt. His research interests include numerical analysis, matrix differential equations, B-Spline functions and fluid dynamics.